

Article

Determination of Dissolution Rates of Ag Contained in Metallurgical and Mining Residues in the $\text{S}_2\text{O}_3^{2-}$ - O_2 - Cu^{2+} System: Kinetic Analysis

Julio C. Juárez Tapia ¹, Francisco Patiño Cardona ², Antonio Roca Vallmajor ³, Aislinn M. Teja Ruiz ^{1,*}, Iván A. Reyes Domínguez ⁴ , Martín Reyes Pérez ¹, Miguel Pérez Labra ¹ and Mizraim U. Flores Guerrero ⁵

¹ Área Académica de Ciencias de la Tierra y Materiales, Universidad Autónoma del Estado de Hidalgo (UAEH), Pachuca de Soto, Hidalgo 42184, Mexico; jcuarez@uaeh.edu.mx (J.C.J.T.); mar_77_mx@hotmail.com (M.R.P.); MIGUELABRA@hotmail.com (M.P.L.)

² Ingeniería en Energía, Universidad Politécnica Metropolitana de Hidalgo, Tolcayuca, Hidalgo 43860, Mexico; franciscopatinocardona@gmail.com

³ Facultat de Química, Departament de Ciència dels Materials i Enginyeria Metallúrgica, Província de Barcelona, Universitat de Barcelona, 08028 Barcelona, Spain; roca@ub.edu

⁴ Catedrático CONACYT-Instituto de Metalurgia, Universidad Autónoma de San Luis Potosí, San Luis Potosí, San Luis Potosí 78210, Mexico; iareyesdo@conacyt.mx

⁵ Área de Electromecánica Industrial, Universidad Tecnológica de Tulancingo, Tulancingo, Hidalgo 43642, México; uri.fg@hotmail.com

* Correspondence: aislinn_teja@uaeh.edu.mx; Tel.: +52-771-7172000 (ext. 2279)

Received: 28 June 2018; Accepted: 18 July 2018; Published: 23 July 2018



Abstract: The materials used to conduct kinetic study on the leaching of silver in the $\text{S}_2\text{O}_3^{2-}$ - O_2 - Cu^{2+} system were mining residues (tailings) from the Dos Carlos site in the State of Hidalgo, Mexico, which have an estimated concentration of Ag = 71 g·ton⁻¹. The kinetic study presented in this paper assessed the effects of the following variables on Ag dissolution rate: particle diameter (d_0), temperature (T), copper concentration [Cu^{2+}], thiosulfate concentration [$\text{S}_2\text{O}_3^{2-}$], pH, [OH^-], stirring rate (RPM), and partial pressure of oxygen (PO_2). Temperature has a favorable effect on the leaching rate of Ag, obtaining an activation energy (E_a) = 43.5 KJ·mol⁻¹ in a range between 288 K (15 °C) and 328 K (55 °C), which indicates that the dissolution reaction is controlled by the chemical reaction. With a reaction order of $n = 0.4$, the addition of [Cu^{2+}] had a catalytic effect on the leaching rate of silver, as opposed to not adding it. The dissolution rate is dependent on [$\text{S}_2\text{O}_3^{2-}$] in a range between 0.02 mol·L⁻¹ and 0.06 mol·L⁻¹. Under the studied conditions, variables d_0 , [OH^-] and RPM did not have an effect on the overall rate of silver leaching.

Keywords: silver leaching; thiosulfate; mining residues; kinetic analysis

1. Introduction

In Mexico, mining accounts for 4% of gross domestic product, which places this country among the top ten world producers of sixteen minerals, among which silver stands out. In 2015, 49% of mining production in Mexico was based on the extraction of precious metals, which represented 7.5 trillion dollars. However, in the last three years there has been a decrease in silver production indices due to the massive exploitation of Au-Ag-Cu-Zn deposits [1]. One way to increase the production of silver is by reprocessing scrap, slag and mining waste that contain economically reasonable amounts of this metal. In the State of Hidalgo, Mexico, due to the extensive mining activity that has lasted approximately 480 years in the mining districts of Pachuca and Mineral del Monte, millions of tons of

mining waste have been accumulated, and are nowadays posing a serious environmental problem [2,3]. In addition, reprocessing these residues presents a challenge for the metallurgical industry because of the presence of quartz and pyrite ores, where the metal values of interest are encapsulated [4].

During the last 30 years, research on the extraction of metal values of gold and silver has been focused on the search for leaching processes alternative to cyanidation, which is a process that has been used for over a century and is considered highly toxic and with a strong impact on the environment [5]. Leaching agents that can substitute cyanide include compounds such as thiocyanate, thiourea and thiosulfate, the last two being the most promising processes, as their application has a lower environmental impact [6–11].

Aylmore and Muir [10] reported that thiosulfate has the advantage of being capable of recovering precious metals and increasing the dissolution rate of metals contained in hard-to-process ores. Since higher dissolution rates mean smaller leaching tanks, investment costs and energy consumption can be reduced [12,13]. The use of thiourea and thiosulfate has been mainly applied to refractory gold and silver ores, in addition to other metals of interest, such as Cu, Pb and Zn, as traditional processes have shown certain deficiencies when treating such minerals [14–17]. As regards to silver leaching, the available published works have been limited, and the kinetic aspects approached show certain inconsistencies. Some of the first research works on silver leaching were conducted by Mohammadi, E. et al. [12], who developed a leaching process at atmospheric pressure using ammonium thiosulfate to recover gold and silver from residues generated during ammoniacal leaching of copper sulfide concentrates. Other studies discussed the chemistry of silver sulfide leaching with solutions of thiosulfates, among which stands out the use of copper sulfate, emphasizing that copper catalyzes the dissolution reaction of the metal values, and assuming that certain equilibrium between the solution and the Cu^+ and Cu^{2+} ions is needed for the extraction to occur [13–19]. Since then several studies have had the aim of explaining how the leaching process with these compounds occurs. Lampinen, M. [20] reported that thiosulfate is a good alternative for leaching gold, noting that the process is favored with the presence of copper ions, increased temperature and by injecting oxygen into the system. Zipperian et al. [21] showed that temperature has a drastic influence on the extraction of silver. At room temperature, they obtained dissolutions of 18% of the precious metal, which increased up to 60% at 60 °C within a period of 3 h.

Thus, it would seem that the thiosulfate system is the most promising for metal extraction, as it can increase the dissolution rate of metals, and because, compared to cyanide, it is a selective method for refractory ores [10,22]. Another alternative that has been studied (in the laboratory) in previous works on the leaching of silver in sulfide or metal form with thiosulfate, is the addition of metal ions Zn^{2+} and Cu^{2+} , where these two oxidize the noble metals while thiosulfate forms stable complexes. In this regard, Juárez et al. [23] and Hernández et al. [24] have used these metal ions in their research, and they found that the process can be a good alternative in the recovery of silver contained in mining residues. They obtained dissolutions higher than 95%, and showed that Zn^{2+} and Cu^{2+} have a catalytic effect on the process by considerably reducing leaching times. In the case of research conducted on the leaching of metal silver using the ammoniacal thiosulfate system, was reported that the process appears to be affected by the formation of copper oxides and sulfides on the surface of the silver particles, thus favoring the precipitation of a considerable amount of this metal in the form of sulfide. Most of the leaching systems with thiosulfate described above have been found to be controlled by the chemical reaction [25]. However, Rivera et al. showed that stirring rate had an effect on the leaching of a silver plate, which was indicative of a strong influence of the oxygen mass transfer in the solid-liquid interface, affecting the reaction rate. This was due to the injection of oxygen and to the geometry of the silver sample [26].

As these examples show, the leaching kinetics of silver with thiosulfate and metal ions as oxidizers has not been widely approached. Moreover, regarding the effect of temperature, optimal concentration of thiosulfate, and effect of catalysts and dissolution atmosphere, several dissimilarities have been published. It is also important to point out that this process has been scarcely used to recover

precious metals contained in mining waste. For this reason, we conducted a kinetic study on the leaching of silver contained in mining residues in the $\text{S}_2\text{O}_3^{2-}$ - O_2 - Cu^{2+} system. We assessed the effect of temperature, reagent concentration, and also of oxygen injection into the system, with the aim of reaching recoveries higher than those obtained with conventional processes, such as cyanidation.

2. Materials and Methods

For this research work we used the Dos Carlos mine dumps from the State of Hidalgo, Mexico, as it is one of the oldest yet least studied areas. It has a total volume of 14.3 million tons, produced in three technologically different periods: grinding-amalgamation, followed by grinding-cyanidation and grinding-flotation-cyanidation [27]. The samples were digested with aqua regia and analyzed using Perkin Elmer Optima 3200 RL ICP-OES spectrometer in order to identify and quantify the elements present in the mine dumps. The concentration of silver was determined by dry route, using the crucible melting cupellation technique, in which the substance is dissolved in a crucible with a reducing flow, to recover the precious metal inside a lead nugget. To determine separately the laws of precious metals in the silver and gold buttons, it was necessary to dissolve them in nitric acid and hydrochloric acid and finally the solutions were analyzed using the ICP-OES technique.

The samples extracted on the field were homogenized and then characterized for identification of oxides by X-ray fluorescence (XRF) using a X-ray sequential spectrophotometer by wavelength dispersion (WDXRF), Philips model PW2400 (Labexchange, Burladingen, Germany). The mineralogical characterization was performed by the X-Ray Diffraction (XRD) technique using a powder diffractometer, Philips model X'Pert and the Scanning Electron Microscopy-Energy-Dispersive X-Ray Spectroscopy (SEM-EDS) technique using a scanning electron microscope, JOEL Model JSM-840 (JEOL, Peabody, MA, USA), which has coupled an oxford dispersive energy spectrometer. The leaching experiments were carried out in a conventional 500 mL glass reactor mounted on a heating plate equipped with stirring rate and temperature controls.

pH was continually measured with an OAKTON pH meter equipped with a gel filled ROSS Ultra pH/ATC Triode electrode that can operate in the 0–14 range. pH adjustments of each experiment were performed by adding a $0.2 \text{ mol} \cdot \text{L}^{-1}$ NaOH solution directly into the reactor. The system's temperature was controlled through a thermometer coupled to the heating plate.

Samples extracted at different times during the leaching experiments were analyzed by atomic absorption spectrophotometry (AAS) using a Perkin Elmer AAnalyst 200 spectrometer to determine the concentration of silver in solution at a given time t .

The fraction of silver was calculated according to the following expression:

$$X_{\text{Ag}} = \frac{[\text{Ag}]_{\text{sol}}}{[\text{Ag}]_{\text{T}}} \quad (1)$$

where: X_{Ag} = Fraction of silver in solution, $[\text{Ag}]_{\text{sol}}$ = concentration of silver at a given time t , $[\text{Ag}]_{\text{T}}$ = total silver concentration, which value corresponds to the amount of silver retained in the particle size selected by the granulometric analysis as the most viable for the kinetic study.

The reagents used for the present work were the following: $\text{Na}_2\text{S}_2\text{O}_3$ (99.9% purity), CuSO_4 (98.9% purity), O_2 (99.9% purity), NaOH (98.8% purity) all Sigma-Aldrich (St. Louis, MO, USA). In order to determine the particle size distribution of the mining residues, a particle size analysis was conducted using a Ro-Tap sieve shaker (Cole-Parmer, Vernon Hills, IL, USA) for 10 min with Taylor sizing sieves and the following mesh sizes: 149, 106, 75, 56, 44, 37, and 25 μm . Sample density was calculated with a pycnometer, using water as immersion liquid. Experimental conditions used in the kinetic study are shown in Table 1.

Table 1. Experimental conditions of the kinetic study.

Parameters	Experimental Conditions
d_0 (μm)	149, 106, 75, 56, 44, 37, 25
$[\text{Cu}^{2+}]$ ($\text{mol}\cdot\text{L}^{-1}$)	0.001, 0.002, 0.003, 0.004, 0.006
$[\text{S}_2\text{O}_3^{2-}]$ ($\text{mol}\cdot\text{L}^{-1}$)	0.02, 0.04, 0.06, 0.08, 0.16, 0.40
T (K)	288, 298, 308, 318, 328
RPM (min^{-1})	250, 350, 450, 550, 650, 750
PO_2	1 atm (excess)
$[\text{OH}^-]$ ($\text{mol}\cdot\text{L}^{-1}$)	1×10^{-9} , 1×10^{-7} , 1×10^{-5} , 1×10^{-3} , 1×10^{-2}

3. Results

3.1. Chemical Characterization

By using XRF determined the elements present in the residues as oxides, obtaining the following chemical composition: SiO_2 (75%), Al_2O_3 (8%), Fe_2O_3 (5%), SO_3 (5%), K_2O (3.4%), CaO (1.5%), Na_2O (0.4%), MgO (0.4%), TiO_2 (0.3%), MnO (0.15%), and P_2O_5 (0.1%).

3.2. Mineralogical Characterization

The X-ray spectrum in Figure 1 shows that silica is the main species (JCPDS No. 01-074-3485), representing the mineralization matrix of these mining residues [27]. Ag appears to be absent in the diffractogram because silver concentration in the residues is under the detection limit of this technique.

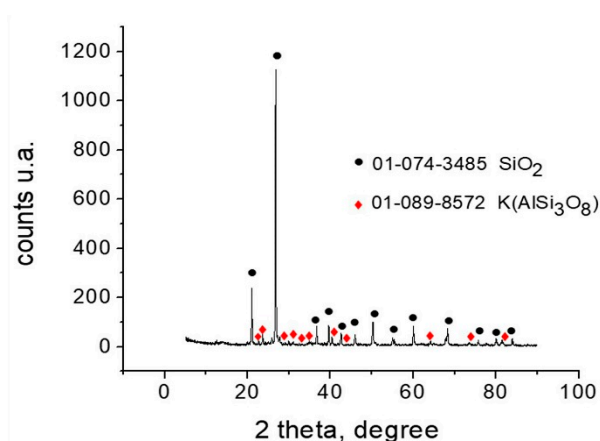


Figure 1. X-ray diffractogram showing the mineralization matrix of the Dos Carlos mine dumps of the State of Hidalgo, Mexico.

Figure 2 shows a micrograph obtained by Reflected light microscopy where the matrix of the mineral sample and the presence of iron sulfides were identified.

The micrograph shown in Figure 3 was obtained by scanning electron microscopy (SEM), in this the main species of quartz and silicates (also obtained through XRD) can be noticed. Figure 4 shows a micrograph obtained by backscattered electrons, whose gray contrast allowed to identify metal particles corresponding to silver sulfide.

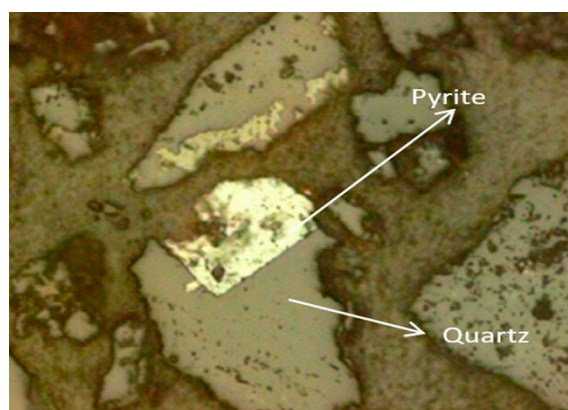


Figure 2. Optical micrograph of the mining residues showing the presence of metal inclusions of pyrite in a quartz matrix.

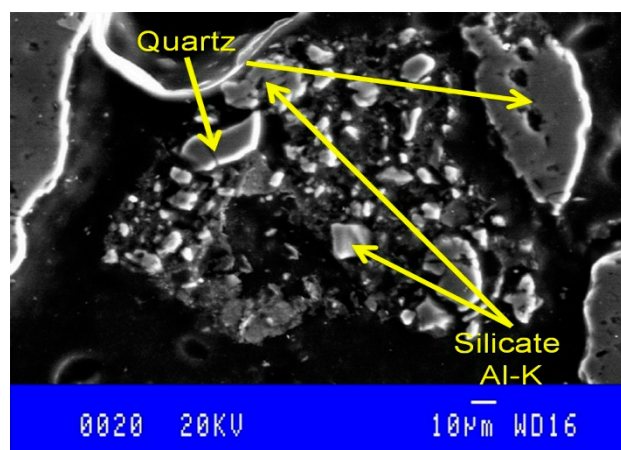


Figure 3. Mixed particles of quartz and silicates. scanning electron microscopy (SEM), secondary electrons.

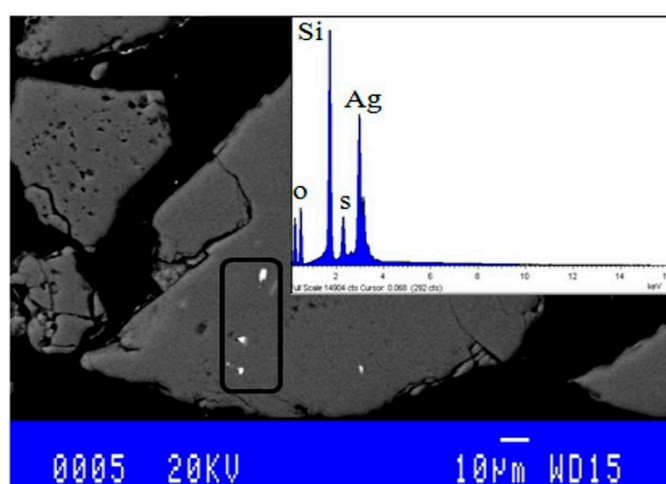


Figure 4. Backscattered electron image and energy dispersive X-ray spectrometry (EDS) spectrum showing the presence of silver sulfide encrusted in a quartz matrix.

3.3. Physical Characterization

The density of the mineral was of 2.57 g/cm³, and the particle size analysis results of the mine dumps are shown in Table 2.

Table 2. Granulometric analysis of the Dos Carlos mine dumps (tailings).

Mesh	Opening (μm)	Ag Retained (g/ton ⁻¹)	Weight (wt %)	Distribution of Ag (wt %)
<100	149	50.13	40	43.51
100–140	106	24.36	53	28
140–200	75	2.81	66	4.01
200–270	56	1.27	63	1.73
270–325	44	1.18	73	1.86
325–400	37	1.20	82	2.12
>400	25	1.65	101	3.53

3.4. Dissolution Curves of Ag and Kinetic Model

In heterogeneous reactions where there is a solid-liquid interface, it is important to consider that the process consists of several stages that include mass transport and the chemical reaction. The variable that allows describing the progress of the reaction is defined as conversion factor (Equation (1)). It represents the amount of reacted mass in relation to the initial mass. In the case of the dissolution of silver, the reaction was monitored by observing the fraction of Ag that passed into the solution (by forming a complex with thiosulfate) in relation to the amount of silver present in the concentrate.

The development of a kinetic study for this kind of non-catalytic reaction, where solid particles are suspended in an active solution, comprises the application of two main models: the progressive conversion model and the unreacted shrinking core model. When the chemical stages occur in shorter times, one can assume that the reagent in heterogeneous reactions is rapidly running out on the solid's surface. The flow of the leaching solution diffuses by unit of time in a perpendicular direction on the surface of the solid particle. In this case, the applied kinetic expression is shown in Equation (2).

$$t/\tau = 1 - 3(1 - X_{Ag})^{2/3} + 2(1 - X_{Ag}) = k_{exp} \cdot t \quad (2)$$

where t is time in min, τ is the total time of the reaction, X_{Ag} is the fraction of silver in solution at a given time t .

When the chemical reaction takes more time compared to phenomena of hydrodynamic nature, no significant concentration gradients appear on the fluid film, so the mechanism of dissolution is controlled by the chemical stages where a low dependence on matter transport, a high sensitivity towards temperature increase, and reaction orders different from the unit are observed [28]. The kinetic equation that describes this process is presented in Equation (3).

$$t/\tau = 1 - (1 - X_{Ag})^{1/3} = k_{exp} \cdot t \quad (3)$$

Figure 5 is an example of how the leaching process of silver with thiosulfates in the proposed medium evolves. The plot shows a rapid dissolution of silver of $X_{Ag} = 0.4$ in the first 12 s, as well the absence of an induction period, which can be attributed to two factors: (1) part of this silver is found released in the mining residues; and [2] selectivity of the complexing agent in relation to silver. Thus, we only observed a progressive conversion period followed by a stabilization period, which indicates the end of the reaction.

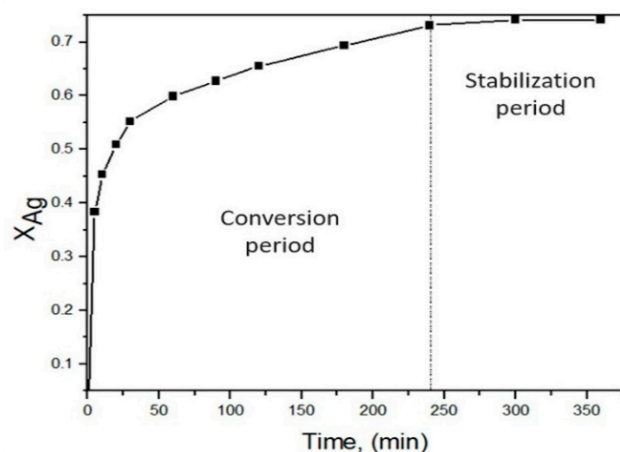


Figure 5. Dissolution curve of silver in the $\text{S}_2\text{O}_3^{2-}\text{-Cu}^{2+}$ system ($V = 0.5 \text{ L}$, 40 g L^{-1} Mineral, $\text{PO}_2 = 1 \text{ atm}$, $\text{pH} = 10$, leaching time = 360 min, $[\text{S}_2\text{O}_3^{2-}] = 0.16 \text{ mol}\cdot\text{L}^{-1}$, $[\text{Cu}^{2+}] = 0.006 \text{ mol}\cdot\text{L}^{-1}$, 298 K (25 °C), $\text{RPM} = 750 \text{ min}^{-1}$).

The data representing X_{Ag} vs. t in Figure 5 were used to assess Equations (4) and (5) (corresponding to control by matter transport and chemical control), which should have a linear behavior, and the obtained slope represents the experimental constant k_{exp} during the progressive conversion period. As seen on Figure 6, the chemical control model is consistent with the linear requirement; therefore, this model can be accepted to describe the dissolution process of silver.

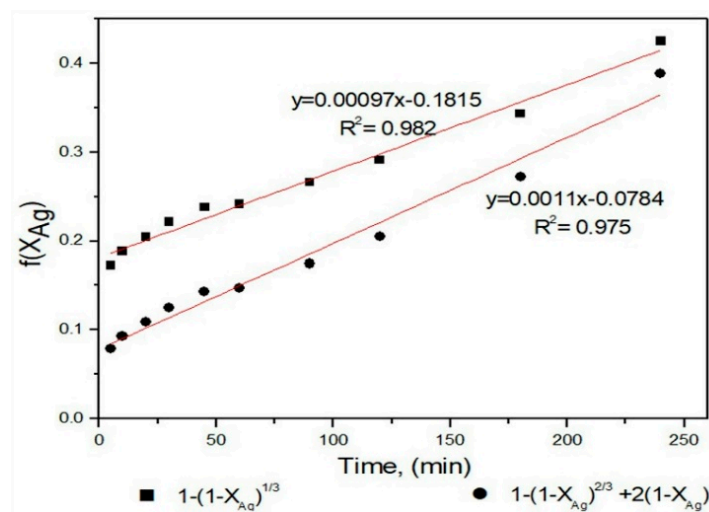


Figure 6. Comparison between the chemical control model and the control-by-transport model for the leaching of silver in the $\text{S}_2\text{O}_3^{2-}\text{-Cu}^{2+}$ system.

3.4.1. Effect of Partial Pressure of Oxygen

For the kinetic study of the leaching of silver in the proposed medium, we assessed the following effects on the dissolution rate of Ag: d_0 , $[\text{Cu}^{2+}]$, $[\text{S}_2\text{O}_3^{2-}]$, $[\text{OH}^-]$, T , RPM and PO_2 . Two experiments were conducted at 0.2 and 1.0 atm of pressure in order to assess the best leaching conditions. Figure 7 shows that the leaching rate of silver is proportional to the partial pressure of oxygen in the system.

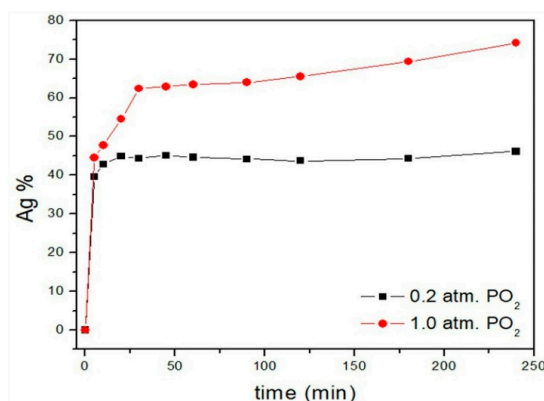


Figure 7. Effect of partial pressure of oxygen on the leaching reaction of silver ($V = 0.5$ L, 40 g L^{-1} Mineral, $\text{pH} = 10$, leaching time = 240 min, $[\text{S}_2\text{O}_3^{2-}] = 0.16\text{ mol}\cdot\text{L}^{-1}$, $[\text{Cu}^{2+}] = 0.006\text{ mol}\cdot\text{L}^{-1}$, 298 K (25 °C), $\text{RPM} = 750\text{ min}^{-1}$).

3.4.2. Particle Size Effect

For the kinetic study of the leaching of silver in the proposed medium, we assessed the following effects on the dissolution rate of Ag: d_0 , $[\text{Cu}^{2+}]$, $[\text{S}_2\text{O}_3^{2-}]$, $[\text{OH}^-]$, T , RPM and PO_2 . In order to determine the effect of the initial particle size, we conducted a series of experiments where the initial particle size was varied, while the other variables were kept constant. According to Equation (4) corresponding to the shrinking core model with chemical control, the constant k_{exp} is defined as follows:

$$k_{\text{exp}} = \frac{2V_m K_q C_A^n}{d_0} \quad (4)$$

where V_m is molar volume, k_q is the chemical rate constant, C_A is the reagent concentration, n is the order of reaction, and d_0 is the initial particle diameter.

Thus, according to Equation (6), a representation of the experimental constants determined at constant concentration, temperature and stirring rate, vs the inverse of particle radius should be linear and pass through the origin, as show the Figure 8.

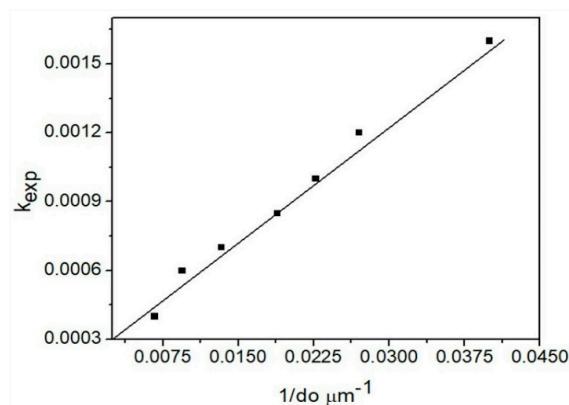


Figure 8. k_{exp} versus the inverse of particle diameter. ($V = 0.5$ L, $40\text{ g}\cdot\text{L}^{-1}$ Mineral, $\text{PO}_2 = 1\text{ atm}$, $\text{pH} = 10$, leaching time = 240 min, $[\text{S}_2\text{O}_3^{2-}] = 0.16\text{ mol}\cdot\text{L}^{-1}$, $[\text{Cu}^{2+}] = 0.006\text{ mol}\cdot\text{L}^{-1}$, 298 K, $\text{RPM} = 750\text{ min}^{-1}$).

3.4.3. Thiosulfate Concentration Effect

The concentration of thiosulfate is another very important variable for this kinetic study, as it is the complexing agent of silver. This variable was studied in an $[\text{S}_2\text{O}_3^{2-}]$ interval = $0.02\text{--}0.40\text{ mol}\cdot\text{L}^{-1}$. At the beginning and for the whole reaction time of each experiment we injected industrial-grade

oxygen in excess. The reaction order was determined by linear regression analysis, plotting the $\log [S_2O_3^{2-}]$ vs the \log of k_{exp} to obtain a straight slope (m). Figure 9 clearly shows two reaction orders for the studied thiosulfate concentrations, i.e., between 0.02, and 0.06 $\text{mol}\cdot\text{L}^{-1}$. A pseudo- order of reaction of $\alpha = 0.4$ was obtained, which indicates that the dissolution rate of silver is dependent on the concentration of thiosulfate. However, for the concentration range between 0.06, and 0.40 $\text{mol}\cdot\text{L}^{-1}$, the order of reaction changed drastically, obtaining in this case a pseudo- order of reaction of $\alpha = 0$, which indicates that, at this concentration range of thiosulfate, the leaching rate of Ag is independent from the concentration of the complexing agent.

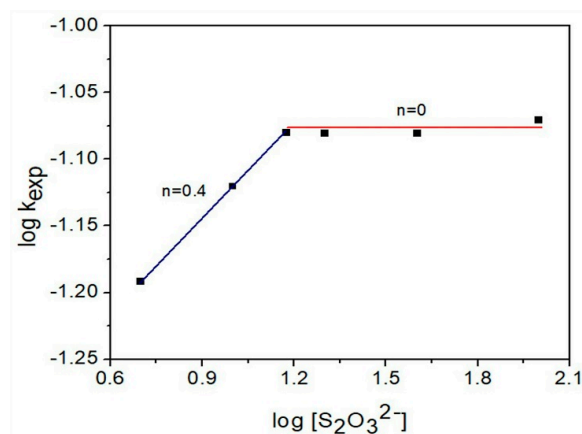


Figure 9. k_{exp} dependence vs. $[S_2O_3^{2-}]$. Reaction order in the concentration range of 0.02 to 0.06 $\text{mol}\cdot\text{L}^{-1}$ ($V = 0.5$ L, 40 $\text{g}\cdot\text{L}^{-1}$ Mineral, $PO_2 = 1$ atm, pH = 10, leaching time = 240 min, $[Cu^{2+}] = 0.006$ $\text{mol}\cdot\text{L}^{-1}$, 298 K (25 °C), RPM = 750 min^{-1}).

3.4.4. Cu^{2+} Concentration Effect

It has been reported that the presence of Cu ions favors the dissolution rate of silver, as well as its maximum release in a leaching solution with sodium thiosulfate [8]. In order to confirm this, we conducted several experiments where concentration of copper was modified in a range between 0.001 $\text{mol}\cdot\text{L}^{-1}$ and 0.006 $\text{mol}\cdot\text{L}^{-1}$, while keeping the other parameters constant. Figure 10 shows $\log k_{exp}$ vs. $\log [Cu^{2+}]$; the straight slope gives a pseudo-order of reaction of $\beta = 0.41$, which indicates that there is a significant dependence of the leaching rate of silver on the presence and increase of the concentration of copper ions in the solution.

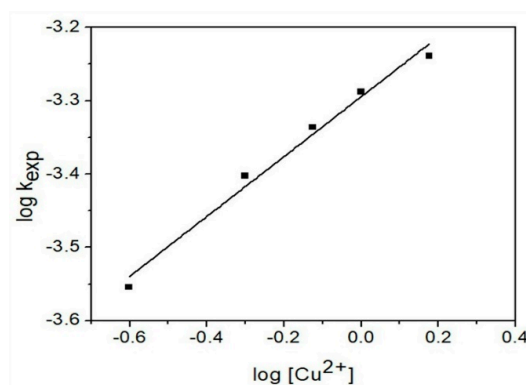


Figure 10. k_{exp} dependence in function of $[Cu^{2+}]$. Reaction order $n = 0.4$. ($V = 0.5$ L, 40 $\text{g}\cdot\text{L}^{-1}$ Mineral, $PO_2 = 1$ atm, pH = 10, leaching time = 240 min, $[S_2O_3^{2-}] = 0.16$ $\text{mol}\cdot\text{L}^{-1}$, 298 K (25 °C), RPM = 750 min^{-1}).

3.4.5. pH Effect

The effect of $[\text{OH}^-]$ on the leaching rate of silver was assessed in a range of pH between 8 and 12, since thiosulfate is more stable in this pH range [25]. As seen on Figure 11.

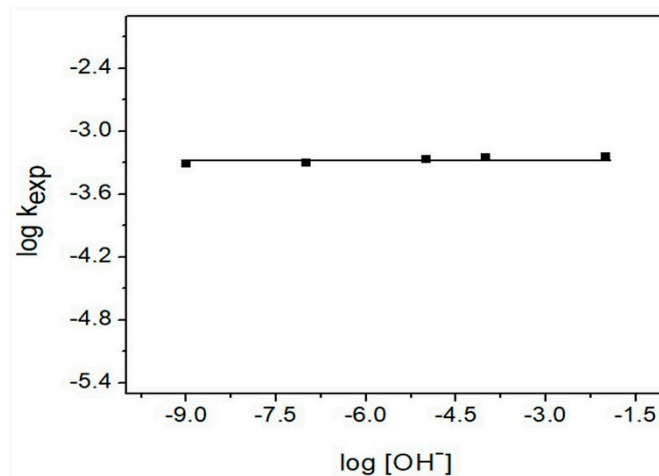


Figure 11. Dependence of $\log k_{\text{exp}}$ in function of $\log [\text{OH}^-]$, obtained reaction order $n = 0$ ($V = 0.5 \text{ L}$, $40 \text{ g}\cdot\text{L}^{-1}$ Mineral, $\text{PO}_2 = 1 \text{ atm}$, leaching time = 240 min, $[\text{S}_2\text{O}_3^{2-}] = 0.16 \text{ mol}\cdot\text{L}^{-1}$, $[\text{Cu}^{2+}] = 0.006 \text{ mol}\cdot\text{L}^{-1}$, 298 K (25 °C), RPM = 750 min^{-1}).

3.4.6. Temperature Effect

The effect of temperature was studied in a range between 288 K (15 °C) and 328 K (55 °C), while the other parameters were kept constant. Figure 12 represents the fraction of leached silver; it was assessed using the shrinking core model with chemical control in function of time for all of the temperatures used.

In order to determine the activation energy of the system, we used the Arrhenius equation [28] shown in Equation (5), where k_q represents the rate constant, k_0 is the frequency factor, E_a is the activation energy, R is the universal gas constant ($8.314 \text{ kJ}\cdot\text{mol}^{-1}$), and T is temperature in K.

$$k_q = k_0 e^{-E_a/RT} \quad (5)$$

Although it is known that the ionization constant of water (k_w) varies considerably along with temperature, this dependence of $[\text{OH}^-]$ on temperature was eliminated with the $k_{\text{exp}}/[\text{OH}^-]^n$ relation according to Equation (4) [29]. By substituting this relation in Equation (6) and applying the natural logarithm, we obtained Equation (6). Equation (12) represents a straight line whose slope corresponds to the $-E_a/R$ value, and the ordinate to the origin corresponds to k_0 .

$$\ln \frac{k_{\text{exp}}}{[\text{OH}^-]^n} = \ln \frac{2V_m k_0}{d_0} - \frac{E_a}{R} \cdot \frac{1}{T} \quad (6)$$

where V_m represent molar molumme, k_0 is the frequency factor and d_0 is particle diameter. The activation energy value is used to obtain the control mechanism. Therefore, we plotted the Napierian logarithm of $k_{\text{exp}}/[\text{OH}^-]^n$ vs. $1/T$, allowing us to determine the activation energy of the system, as shown in Figure 13.

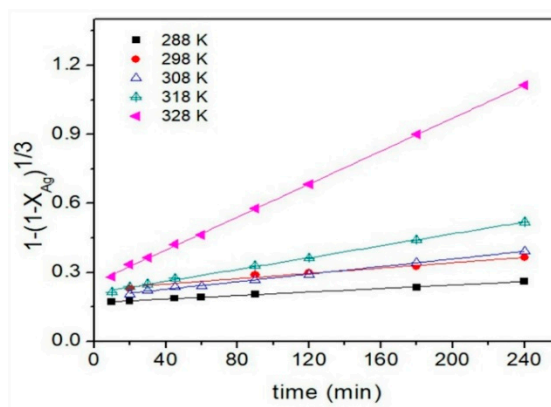


Figure 12. Assessment of the application of the chemical control model on the conversion values of Ag in function of time for the study of the temperature effect in the $\text{S}_2\text{O}_3^{2-}$ - O_2 system, ($V = 0.5 \text{ L}$, $40 \text{ g}\cdot\text{L}^{-1}$ Mineral, $\text{PO}_2 = 1 \text{ atm}$, $\text{pH} = 10$, leaching time = 240 min, $[\text{S}_2\text{O}_3^{2-}] = 0.16 \text{ mol}\cdot\text{L}^{-1}$, $[\text{Cu}^{2+}] = 0.006 \text{ mol}\cdot\text{L}^{-1}$, 298 K (25 °C), $\text{RPM} = 750 \text{ min}^{-1}$).

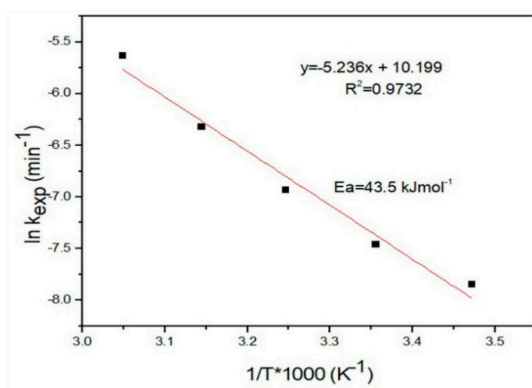


Figure 13. Dependence of $\ln k_{\text{exp}}$ vs temperature. Calculated activation energy, $E_a = 43.5 \text{ kJ}\cdot\text{mol}^{-1}$.

3.4.7. Stirring Rate Effect

In order to know if there are changes in the leaching rate of silver when the stirring rate is modified, we conducted a number of experiments in an interval between 250 min^{-1} and 750 min^{-1} , keeping the other variables constant. In Figure 14, one can observe that the global rate of the reaction does not depend on the stirring rate, since the values of k_{exp} were constant in all the experiments ($k_{\text{exp}} \approx 0.0585 \text{ min}^{-1}$).

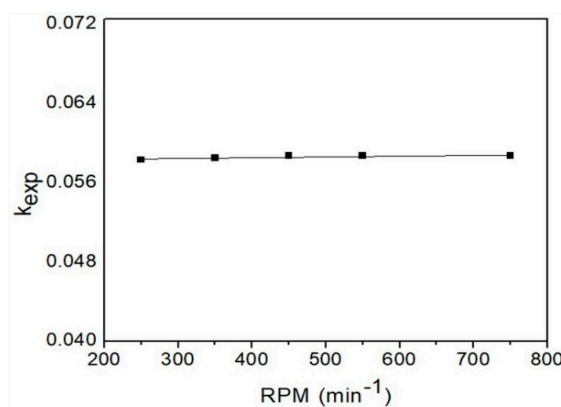


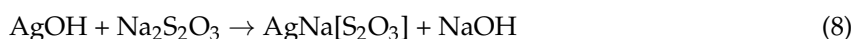
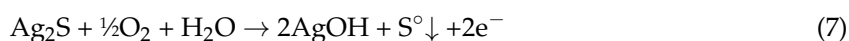
Figure 14. Dependence of k_{exp} in function of stirring rate.

4. Discussion

Results of the chemical characterization, which was carried out by X-ray fluorescence (XRF) and by the cupellation technique, showed similar silver contents. We could establish that the obtained concentrations of Ag in the mine dumps were of the order of $75 \text{ g}\cdot\text{ton}^{-1}$ and $71 \text{ g}\cdot\text{ton}^{-1}$ respectively. The Figure 1 is consistent with the results obtained by XRF. It is also possible to notice the presence of some feldspars, such as potassium silicate (JCPDS No. 01-089-8572), which is one of the secondary minerals formed by supergene oxidation. It is common in small amounts in veins associated with silver-rich ores [4,30].

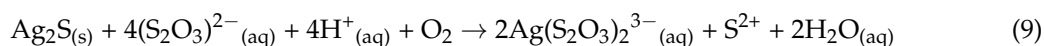
As regards the mineralogical characterization, the technique of Reflected light microscopy identified abundant fragments of quartz crystals, silicates and scarce metal mineralization. Such mineralization is composed mainly of base metal sulfides that make up the ore [31–33] such as pyrite (FeS_2) associated with quartz (SiO_2), as shown in the micrograph on Figure 2. To complete the characterization study, the mineral was analyzed by scanning electron microscopy (SEM) along with energy dispersive X-ray spectrometry (EDS). Microanalyses performed on particles with a coarse aspect showed a mixed composition, as observed in Figure 3. Upon sample analysis with backscattered electrons, we were able to see that silver is present in the form of argentite (Ag_2S) encrusted in a quartz matrix, as observed in Figure 4. This has previously been reported by Geyne A.R. and Fries C. [4]. According to the results obtained by granulometric analysis of the Dos Carlos mine dumps, it can be observed that the highest retained weight percentage (50.13%) and distribution of silver (43.51%) were obtained with mesh size 100 ($149 \mu\text{m}$). Therefore, this particle size (100) was used in all of the experiments for the kinetic study.

Determining the stoichiometry of the reaction is challenging due to the complexity of the mineralization contained in the Dos Carlos tailings. Thus, we used theoretical stoichiometry based on the characterization results in order to estimate the presence of silver in the mine dumps as silver sulfide. The proposed equations are the following:

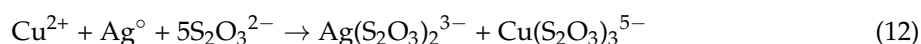
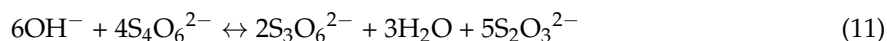
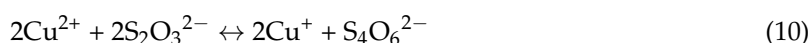


The kinetic study of silver leaching in $\text{S}_2\text{O}_3^{2-}$ - O_2 - Cu^{2+} medium revealed that the recovery of Ag increases, from 46% at 0.2 atm, to 74% when using 1 atm of gas pressure at the same reaction time of 240 min (Figure 7). Since there were no significant changes in the dissolution rates at more than 1 atm of O_2 pressure (O_2 is clearly in excess), we decided to use 1 atm pressure in all the experiments for practical reasons. In the study of Particle size effect can be noted that the experimental constant obtained in experiments with different initial particle sizes is inversely proportional to particle diameter ($k_{\text{exp}} \cdot \alpha \cdot (1/d_0)$); thus, the leaching reaction of silver is consistent with the proposed model (Figure 8). In addition, we could confirm that, as particle size decreases, the leaching rate of silver increases. This is due to the presence of a larger surface area on the silver particles that are in contact with the leaching agent [26]. Moreover, the thiosulfate concentration effect reported an apparent change in the reaction occurred because, at low thiosulfate concentrations, the leaching rate of silver depends on the partial pressure of oxygen, and on a high consumption of complexing agent, which, possibly, is not present in enough quantities to sustain the dissolution reaction (Figure 9). Nonetheless, at concentrations ranging from $0.06 \text{ mol}\cdot\text{L}^{-1}$ to $0.40 \text{ mol}\cdot\text{L}^{-1}$, a saturation of the complexing agent in the solution was observed (it was found in excess) that keeps the leaching rate constant. Thus, the leaching rate depends only on the concentration of dissolved oxygen.

The increase of the leaching rate in the presence of Cu^{2+} is due to a parallel reaction to the oxidation of silver. The leaching reaction of Ag in the O_2 - $\text{S}_2\text{O}_3^{2-}$ system without a catalyst basically depends on the oxygen dissolved in the system, as shown in Equation (9):



This is different from the reaction in the presence of $[\text{Cu}^{2+}]$, where the reduction of Cu^{2+} to Cu^+ causes the Ag° to oxidize to Ag^+ as described in Equations (10)–(12).



This confirms that, in the presence of oxygen and copper ions, leaching with thiosulfate has a favorable effect on the reaction (Figure 10), with up to 30% increase compared to the same process without using copper [26,34,35]. The maximum recovery of silver was 74.4% with the addition of $0.25 \text{ (g}\cdot\text{L}^{-1})$ Cu^{2+} at room temperature, while without copper the Ag recoveries were of 43% at the same conditions of the reaction. While the study of pH effect allowed the calculation of a reaction order of $n = 0$ was obtained, which indicates that the leaching rate does not depend on the $[\text{OH}^-]$ values (Figure 11); this is consistent with previous works by Rivera et al. [26], who explained that the degradation of thiosulfate occurs preferably in the pH range of $8 < \text{pH} < 12$.

The Figure 12 shows the strong influence of temperature on the dissolution rate. The plot demonstrates straight lines whose slopes represent the experimental rate constants (k_{exp}), where, as temperature is increased, the fraction of silver in solution rises as well. There is a moderate increase from 288 K (15 °C) to 318 K (45 °C), while upon reaching the highest temperature of 323K (50 °C), the fraction of leached silver increases drastically until reaching 0.96 in a time of 240 min. The obtained E_a value was $43.5 \text{ kJ}\cdot\text{mol}^{-1}$ (Figure 13) which indicates that the chemical reaction is the controlling mechanism of the leaching process of silver in the studied system [36]. Finally, the study of Stirring rate effect the transport of matter in the solid-liquid interface has no significant effect on the dissolution rate when modifying the range of revolutions per minute (Figure 14). It can be confirmed that the slow, controlling stage, is the chemical reaction.

Due to the obtained value of $>40 \text{ kJ}\cdot\text{mol}^{-1}$ for the activation energy, which established a control by chemical reaction, and to the fact that k_{exp} was inversely proportional to the initial particle diameter and passes through the origin, it was possible to confirm that the shrinking core model with chemical control is the one that satisfactorily describes the leaching process of silver in $\text{S}_2\text{O}_3^{2-}$ - Cu^{2+} . Therefore, by combining and arranging Equations (3)–(5), it is possible to obtain a general kinetic model that describes the Ag dissolution of the metallurgical residues in the $\text{S}_2\text{O}_3^{2-}$ - Cu^{2+} system, taking into consideration that the O_2 concentration in the system remains constant:

$$1 - (1 - X_{\text{Ag}})^{\frac{1}{3}} = \frac{V_m K_o}{r_o} e^{-\frac{E_a}{RT}} [\text{S}_2\text{O}_3^{2-}]^\alpha [\text{Cu}^{2+}]^\beta t \quad (13)$$

where α and β correspond to pseudo- orders of reaction related to $[\text{S}_2\text{O}_3^{2-}]$ and $[\text{Cu}^{2+}]$ respectively, and $\alpha + \beta = n$ is the global order of reaction for the studied system. By substituting the obtained kinetic parameters of k_o , E_a , and n in Equation (13), the following expression was obtained:

$$1 - (1 - X_{\text{Ag}})^{\frac{1}{3}} = 1.6 \times 10^4 e^{-\frac{43,5000}{RT}} [\text{S}_2\text{O}_3^{2-}]^{0.4} [\text{Cu}^{2+}]^{0.4} t \quad (14)$$

Equation (14) shows the effect of time, and of $\text{S}_2\text{O}_3^{2-}$ and Cu^{2+} concentrations on the fraction of silver that is transformed into product, which is valid in the temperature range between 288 K (15 °C) and 328 K (55 °C), and in concentrations ranging from 0.02 to $0.06 \text{ mol}\cdot\text{L}^{-1}$ $\text{S}_2\text{O}_3^{2-}$ and 0.001 to $0.006 \text{ mol}\cdot\text{L}^{-1}$ Cu^{2+} .

5. Conclusions

Results of the characterization of the mine dumps showed that silver is found in the form of sulfide encrusted in quartz and pyrite matrixes. The Ag concentration is of the order of $71 \text{ g}\cdot\text{ton}^{-1}$. The main

non-metal mineral phase (determined by XRD) was quartz, while the reflected light microscope and EDS microanalysis revealed that the most abundant metal species in the mine dumps is pyrite.

The dissolution rate is influenced by concentrations of thiosulfate in the $0.02\text{--}0.06\text{ mol}\cdot\text{L}^{-1}$ range, with saturation of the complexing agent observed from $0.06\text{ mol}\cdot\text{L}^{-1}$, which causes the leaching rate to stay constant at higher concentration values. The pseudo- order of reaction with respect to the concentration of copper ions was $n = 0.4$, which suggests a catalytic effect, since an increase in the leaching rate of silver was observed. In addition, the partial pressure of oxygen dissolved in the system with thiosulfates has a favorable effect on the leaching rate, with an increase of up to 30% when increasing gas pressure from 0.2 atm to 1.0 atm.

Since temperature was found to have a drastic effect on the leaching rate of silver ($E_a = 43.5\text{ kJ}\cdot\text{mol}^{-1}$), while modification of the stirring rate was not found to have such an effect, it was demonstrated that the matter chemical stages evolve in shorter time intervals, compared to the transport stages. This was confirmed through the adjustment made on the shrinking core model with chemical control ($k_{\text{exp}}\cdot t = 1 - (1 - X)^{1/3}$). The maximum silver recovery was of (96.8%) under the following experimental conditions: $[\text{S}_2\text{O}_3^{2-}] = 0.08\text{ mol}\cdot\text{L}^{-1}$, $[\text{Cu}^{2+}] = 0.006\text{ mol}\cdot\text{L}^{-1}$, RPM = 650 min^{-1} , $T = 328\text{ K}$ ($55\text{ }^\circ\text{C}$), $\text{PO}_2 = 1\text{ atm.}$, pH = 10 and $t = 240\text{ min.}$

According to the results obtained, the present work suggests that there is a real possibility of using the $\text{S}_2\text{O}_3^{2-}\text{--O}_2$ system, adding copper ions (II) as an oxidizing reagent, to improve the kinetic conditions of the leaching process. The proposed system represents a reasonably viable alternative, since silver is present in real refractory waste from the mining industry, making this an innovative method.

Author Contributions: J.C.J.T. designed and performed the experiments and wrote the paper; F.P.C. realized the chemical characterization; A.R.V. performed the cupellation technique and the characterization by XRF and MEB-EDS; A.M.T.R. and I.A.R.D. conducted the discussion of results and wrote the paper; M.R.P. and M.P.L. performed the characterization by DRX and the granulometric analysis; M.U.F.G. realized the characterization by MOP.

Funding: The authors would like to thank the Universidad Autónoma del Estado de Hidalgo (Autonomous University of the State of Hidalgo) and the Consejo Nacional de Ciencia y Tecnología, CONACyT (National Council for Science and Technology), of the Mexican government for the funding of the present work.

Acknowledgments: The authors would like to thank the University of Barcelona for their technical-scientific services and for their collaboration in this piece of work.

Conflicts of Interest: The authors declare no conflicts of interest.

References

1. Lopez, C. México: Política en Materia Minera. (Diálogo Unión Europea-América Latina Sobre Materias Primas 2014). Available online: europa.eu/geninfo/query/index.do?queryText=plata&query_source=GROWTH&summary=summary&more_options_source=restricted&more_options_date=*%&more_options_date_from=&more_options_date_to=&more_options_language=es&more_options_f_formats=*&swlang=en (accessed on 14 July 2018).
2. Patiño, F.; Hernández, J.; Flores, M.U.; Reyes, I.A.; Reyes, M.; Juárez, J.C. Characterization and Stoichiometry of the Cyanidation Reaction in NaOH of Argentinian Waste Tailings of Pachuca, Hidalgo, México. In *Characterization of Minerals, Metals, and Materials*; Springer: Cham, Switzerland, 2016; Volume 145, pp. 355–362, ISBN 978-1-119-26439-2.
3. Flores, J.; Hernández, J.; Rivera, I.; Reyes, M.I.; Cerecedo, E.; Reyes, M.; Salinas, E.; Guerrero, M. Study of the Effect of Surface Liquid Flow during Column Flotation of Mining Tailing of the Dos Carlos Dam. In *Characterization of Minerals, Metals, and Materials*; Springer: Cham, Switzerland, 2017; Volume 146, pp. 787–798.
4. Teja Ruiz, A.M.; Juarez Tapia, J.C.; Reyes Perez, M.; Hernandez Cruz, L.E.; Flores, M.U.; Reyes, I.A.; Perez Labra, M.; Moreno, R. Characterization and Leaching Proposal of Ag(I) from a Zn Concentrate in an $\text{S}_2\text{O}_3^{2-}\text{--O}_2$ Medium. In *Characterization of Minerals, Metals, and Materials*; Springer: Cham, Switzerland, 2017; Volume 146, pp. 567–575.

5. Hilson, G.; Monhemius, J. Alternatives to cyanide in the gold mining industry: What prospects for the future. *J. Clean. Prod.* **2015**, *14*, 1158–1167. [[CrossRef](#)]
6. Hernandez, J.; Patino, F.; Rivera, I.; Reyes, I.A.; Flores, M.U.; Juarez, J.C.; Reyes, M. Leaching kinetics in cyanide media of Ag contained in the industrial mining-metallurgical wastes in the state of Hidalgo, Mexico. *Int. J. Min. Sci. Technol.* **2014**, *24*, 689–694. [[CrossRef](#)]
7. Briones, R.; Lapidus, G.T. The leaching of silver sulfide with the thiosulfate–ammonia–cupric ion system. *Hydrometallurgy* **1998**, *50*, 243–260. [[CrossRef](#)]
8. Alvarado-Macías, G.; Fuentes-Aceituno, J.C.; Nava-Alonso, F. Study of silver leaching with the thiosulfate-nitrite-copper alternative system: Effect of thiosulfate concentration and leaching temperature. *Miner. Eng.* **2016**, *86*, 140–148. [[CrossRef](#)]
9. Alonso, A.R.; Lapidus, G.T.; González, I. A strategy to determine the potential interval for selective silver electrodeposition from ammoniacal thiosulfate solutions. *Hydrometallurgy* **2007**, *85*, 144–153. [[CrossRef](#)]
10. Aylmore, M.G.; Muir, D.M. Thiosulfate leaching of gold—A review. *Miner. Eng.* **2001**, *14*, 135–174. [[CrossRef](#)]
11. Abbruzzese, C.; Fornari, P.; Massidda, R.; Veglio, F.; Ubaldini, S. Thiosulphate leaching for gold hydrometallurgy. *Hydrometallurgy* **1995**, *39*, 265–276. [[CrossRef](#)]
12. Mohammadi, E.; Pourabdoli, M.; Ghobeiti-Hasab, M.; Heidarpour, A. Ammoniacal thiosulfate leaching of refractory oxide gold ore. *Int. J. Miner. Process.* **2017**, *164*, 6–10. [[CrossRef](#)]
13. Ubaldini, S.; Fornari, P.; Massidda, R.; Abbruzzese, C. An innovative thiourea gold leaching process. *Hydrometallurgy* **1998**, *48*, 113–124. [[CrossRef](#)]
14. Alonso-Gómez, A.; Lapidus, G. Inhibition of lead solubilization during the leaching of gold and silver in ammoniacal thiosulfate solutions (effect of phosphate addition). *Hydrometallurgy* **2009**, *99*, 89–96. [[CrossRef](#)]
15. Deutsch, J.L.; Dreisinger, D.B. Silver sulfide leaching with thiosulfate in the presence of additives part I: Copper–ammonia leaching. *Hydrometallurgy* **2013**, *137*, 156–164. [[CrossRef](#)]
16. Feng, D.; Van Deventer, J.S.J. Ammoniacal thiosulphate leaching of gold in the presence of pyrite. *Hydrometallurgy* **2006**, *82*, 126–132. [[CrossRef](#)]
17. Solis-Marcial, O.J.; Lapidus, G.T. Chalcopyrite leaching in alcoholic acid media. *Hydrometallurgy* **2014**, *147–148*, 54–58. [[CrossRef](#)]
18. Xu, B.; Yang, Y.; Jiang, T.; Li, Q.; Zhang, X.; Wang, D. Improved thiosulfate leaching of a refractory gold concentrate calcine with additives. *Hydrometallurgy* **2015**, *152*, 214–222. [[CrossRef](#)]
19. Grosse, A.C.; Dicoski, G.W.; Shaw, M.J.; Haddad, P.R. Leaching and recovery of gold using ammoniacal thiosulfate leach liquors (a review). *Hydrometallurgy* **2003**, *69*, 1–21. [[CrossRef](#)]
20. Lampinen, M.; Laari, A.; Turunen, I. Ammoniacal thiosulfate leaching of pressure oxidized sulfide gold concentrate with low reagent consumption. *Hydrometallurgy* **2015**, *151*, 1–9. [[CrossRef](#)]
21. Zipperian, D.; Raghavan, S.; Wilson, J.P. Gold and silver extraction by ammoniacal thiosulfate leaching from a rhyolite ore. *Hydrometallurgy* **1988**, *19*, 361–378. [[CrossRef](#)]
22. Patiño, F.; Reyes, I.A.; Flores, M.U.; Pandiyan, T.; Roca, A.; Reyes, M.; Hernández, J. Kinetics modeling and experimental design of the sodium arsenojarsite decomposition in alkaline media: Implications. *Hydrometallurgy* **2013**, *137*, 115–125. [[CrossRef](#)]
23. Juárez, J.C.; Rivera, I.; Patiño, F.; Reyes, M. Efecto de la Temperatura y Concentración de Tiosulfatos sobre la Velocidad de Disolución de Plata contenida en Desechos Mineros usando Soluciones $S_2O_3^{2-}$ – O_2 – Zn^{2+} . *Inf. Tecnol.* **2012**, *18*, 1–12. [[CrossRef](#)]
24. Hernández, J.; Rivera, I.; Patiño, F.; Juárez, J.C. Estudio Cinético de la Lixiviación de Plata en el Sistema $S_2O_3^{2-}$ – O_2 – Cu^{2+} Contenido en Residuos Minero-Metalúrgicos. *Inf. Tecnol.* **2012**, *16*, 1–10. [[CrossRef](#)]
25. Skoog, A.D.; West, D.M. *Analytical chemistry an Introduction*, 1st ed.; Reverté: Barcelona, Spain, 2002; pp. 444–445, ISBN 8429175113.
26. Rivera, I.; Patiño, F.; Roca, A.; Cruells, M. Kinetics of metallic silver leaching in the O_2 –thiosulfate system. *Hydrometallurgy* **2015**, *156*, 63–70. [[CrossRef](#)]
27. Teja-Ruiz, A.M.; Juárez-Tapia, J.C.; Reyes-Domínguez, I.A.; Hernández- Cruz, L.E.; Reyes-Pérez, M.; Patiño-Cardona, F.; Flores-Guerrero, M.U. Kinetic Study of Ag Leaching from Arsenic Sulfosalts in the $S_2O_3^{2-}$ – O_2 – $NaOH$ System. *Metals* **2017**, *7*, 411. [[CrossRef](#)]
28. Levenspiel, O. *Ingeniería de las Reacciones Químicas*, 2nd ed.; Reverté: Barcelona, Spain, 2002; pp. 397–441, ISBN 968-18-5860-3.

29. Tanda, B.C.; Eksteen, J.J.; Oraby, E.A. Kinetics of chalcocite leaching in oxygenated alkaline glycine solutions. *Hydrometallurgy* **2018**, *178*, 264–273. [[CrossRef](#)]
30. Moreno-Tovar, R.; Téllez-Hernández, J.; Monroy-Fernández, M.G. Evaluación geoquímica de residuos mineros (jales o colas) de mineralización de tipo epitermal, Hidalgo, México. *Rev. Geol. Am. Cent.* **2009**, *41*, 79–98, ISSN: 0256-7024.
31. Moreno-Tovar, R.; Monroy, M.G.; Castañeda, E.P. Influencia de los minerales de los jales en la bioaccesibilidad de arsénico, plomo, zinc y cadmio en el distrito minero Zimapán, México. *Rev. Geol. Am. Cent.* **2012**, *28*, 3, ISSN: 0188-4999.
32. Asamoah, R.A.; Skinner, W.; Addai-Mensah, J. Alkaline cyanide leaching of refractory gold flotation concentrates and bio-oxidised products: The effect of process variables. *Hydrometallurgy* **2018**, *179*, 79–93. [[CrossRef](#)]
33. Melo, P.; Halmenschlager, P.; Veit, H.M.; Bernardes, A.M. Leaching of gold and silver from printed circuit board of mobile phones. *Rev. Esc. Minas* **2015**, *68*, 61–68. [[CrossRef](#)]
34. Sitando, O.; Senanayake, G.; Dai, X.; Nikoloski, A.N.; Breuer, P. A review of factors affecting gold leaching in non-ammoniacal thiosulfate solutions including degradation and in-situ generation of thiosulfate. *Hydrometallurgy* **2018**, *178*, 151–175. [[CrossRef](#)]
35. Langhans, J.W., Jr.; Lei, K.P.V.; Carnahan, T.G. Copper-catalyzed thiosulfate leaching of low-grade gold ores. *Hydrometallurgy* **1992**, *29*, 191–203. [[CrossRef](#)]
36. Ballester, A.; Felipe Verdeja, L.; Sancho, J. *Metallurgia Extractiva Vol. I Fundamentos*, 2nd ed.; Síntesis: Barcelona, Spain, 2000; pp. 37–67, ISBN 9788477388029.



© 2018 by the authors. Licensee MDPI, Basel, Switzerland. This article is an open access article distributed under the terms and conditions of the Creative Commons Attribution (CC BY) license (<http://creativecommons.org/licenses/by/4.0/>).